

A Method for Sea Surface Wind Field Retrieval from SAR Image Mode Data

SHAO Weizeng¹⁾, SUN Jian²⁾,*, GUAN Changlong²⁾, and SUN Zhanfeng¹⁾

1) Marine Science and Technical College, Zhejiang Ocean University, Zhoushan 316000, P. R. China

2) Physical Oceanography Laboratory, Ocean University of China, Qingdao 266100, P. R. China

(Received April 5, 2012; revised September 18, 2012; accepted October 12, 2013)

© Ocean University of China, Science Press and Springer-Verlag Berlin Heidelberg 2014

Abstract To retrieve wind field from SAR images, the development for surface wind field retrieval from SAR images based on the improvement of new inversion model is present. Geophysical Model Functions (GMFs) have been widely applied for wind field retrieval from SAR images. Among them CMOD4 has a good performance under low and moderate wind conditions. Although CMOD5 is developed recently with a more fundamental basis, it has ambiguity of wind speed and a shape gradient of normalized radar cross section under low wind speed condition. This study proposes a method of wind field retrieval from SAR image by combining CMOD5 and CMOD4. Five VV-polarisation RADARSAT2 SAR images are implemented for validation and the retrieval results by a combination method (CMOD5 and CMOD4) together with CMOD4 GMF are compared with QuikSCAT wind data. The root-mean-square error (RMSE) of wind speed is 0.75 m s^{-1} with correlation coefficient 0.84 using the combination method and the RMSE of wind speed is 1.01 m s^{-1} with correlation coefficient 0.72 using CMOD4 GMF alone for those cases. The proposed method can be applied to SAR image for avoiding the internal defect in CMOD5 under low wind speed condition.

Key words SAR; surface wind retrieval; geophysical model function; CMOD4; CMOD5

1 Introduction

In recent years, particular efforts have been made to derive surface wind fields over the ocean from synthetic aperture radar (SAR) images. Due to the high resolution of SAR images, the surface wind field retrieved from SAR images has the ability to describe the detailed structure of the atmospheric phenomena (Gerling, 1986; Alpers and Brummer, 1994; Stoffelen and Anderson, 1992; Shimada and Kawamura, 2004).

Through analyzing SAR images, wind field is calculated from the inversion of the Geophysical Model Function (GMF) that indicates the relationship of the observed normalized radar cross section (NRCS) and the corresponding sea surface wind vector combined with radar parameters. Because most common expressions of atmospheric phenomena occurring in the marine boundary layer can be manifested using C-band electromagnetic wave, CMOD models are maturely developed aimed at C-band electromagnetic wave. At present, there are several CMOD models developed by different researchers. The research comparing NRCS with measured wind vectors and numerical model predictions of wind vector leads to the development of the CMOD4 model function (Stof-

felen and Anderson, 1992, 1997a, 1997b). In parallel, an analogous CMOD-IFR2 was developed (IFREMER, 1996). Recently after collecting more ERS-2 SAR data and wind field model data from European Centre for Medium-Range Weather Forecasts (ECMWF), CMOD5 which corrects some deficiencies of the currently widely used CMOD4 GMF was developed (Hersbach, 2003; Hersbach *et al.*, 2007). However, as a wind vector has two components: wind speed and direction, the derivation of wind vector by inverting the GMF remains a problem.

To solve it, different types of procedures are developed, which are divided into three categories (Type I, II, III) in wind direction.

In procedure of type I, it is important to estimate wind direction by a priori knowledge of the wind direction information. Wind direction can sometimes be extracted directly from spatial patterns visible on SAR scenes (Alpers and Brummer, 1994), such as using two-dimensional spectrum (Wacherman *et al.*, 1996; Fetterer *et al.*, 1998), or the local gradient method (Koch, 2004). However, ancillary data is required to resolve the 180° ambiguity using the external wind vector such as ECMWF or QuikSCAT data. Once the wind direction has been estimated, the wind speed is inverted by means of GMF. Note that the retrieval results through this procedure are not adequate enough for SAR image where there is no apparent wind streak.

The procedure of type II is based on the statistical wind

* Corresponding author. Tel: 0086-532-66786228

E-mail: sunjian77@ouc.edu.cn

speed algorithm (SWRA) (Portabella *et al.*, 2002). The procedure combines the SAR backscatter information with the background wind field such as that from a high resolution limited area model. The key of this procedure is building a cost function which has wind vector and backscatter measurement. The retrieved wind vector is estimated by minimizing the cost function using the maximum likelihood method.

Procedure of type III is based on the principle operated by the SAR system in the azimuth channel due to the orbital motion of the sea water particles (Kerbaol *et al.*, 1998). In this procedure, the key step is the estimation of azimuthally cut-off wavelength from the image spectrum which is directly related to wind speed. After wind speed is obtained, the wind direction can be retrieved directly using an inversion procedure based on GMF such as CMOD4 or CMOD5.

In this paper, it is found that the newest GMF function, CMOD5, has ambiguity of wind speed and shape gradient of NRCS under low wind speed condition. A practical method is presented using two existing CMOD models (CMOD4, CMOD5) for retrieving wind field under low wind speed condition. In Section 2 the description of data information involved in this paper is introduced. In Section 3, there is an introduction that elaborates the method proposed in this study and five VV-polarisation RADARSAT2 SAR images around the coast of China are processed for wind field retrieval by combination of CMOD5 and CMOD4. In Section 4, the results of SAR-derived surface wind fields are compared to the QuikSCAT scatterometer wind data. The conclusion is given in Section 5.

2 Data

We take the ECMWF with $1.5^{\circ} \times 1.5^{\circ}$ resolution performed second reanalysis called ERA-40 covering 45

years from 1957 to 2011 at the four synoptic times 00:00, 06:00, 12:00 and 18:00 UTC each day. The QuikSCAT data used in this study is from Physical Oceanography Distributed Active Archive Center and swath data on a 0.25° grid are used.

RADARSAT2 SAR is a newly C-band space-borne synthetic aperture radar, which was launched in 2007. In our study, all of the VV-polarisation RADARSAT2 SAR images were taken in 2009 around Hainan Island in China. It is necessary to note that there are several hours difference between the five collected VV-polarisation RADARSAT2 SAR images and QuikSCAT products which could cause bigger error between inverted results and QuikSCAT products. The main technique parameters and acquisition time of all RADARSAT2 SAR images used in this study is shown in Table 1. A case quick-look of RADARSAT2 SAR images taken on March 10th at 10:49 UTC in 2009 and the geographic location of the RADARSAT2 SAR image is shown in Fig.1. Note that the levels are annotated by water depth and the black frame area is matched the full size of SAR image.

Table 1 The main technique parameters and acquisition time of all RADARSAT2 SAR images used in this study

Sensor	RADARSAT2 SAR
Wave length	5.3 cm
Swath width	100 km
Incidence angle	20° – 50°
Polarisation	VV
Resolution (Azimuth×Range)	25×25 m
Location	Hainan Island, China
	2009-02-21 10:45
	2009-03-03 10:53
Data and time	2009-03-08 22:32
	2009-03-10 10:49
	2009-03-17 10:45

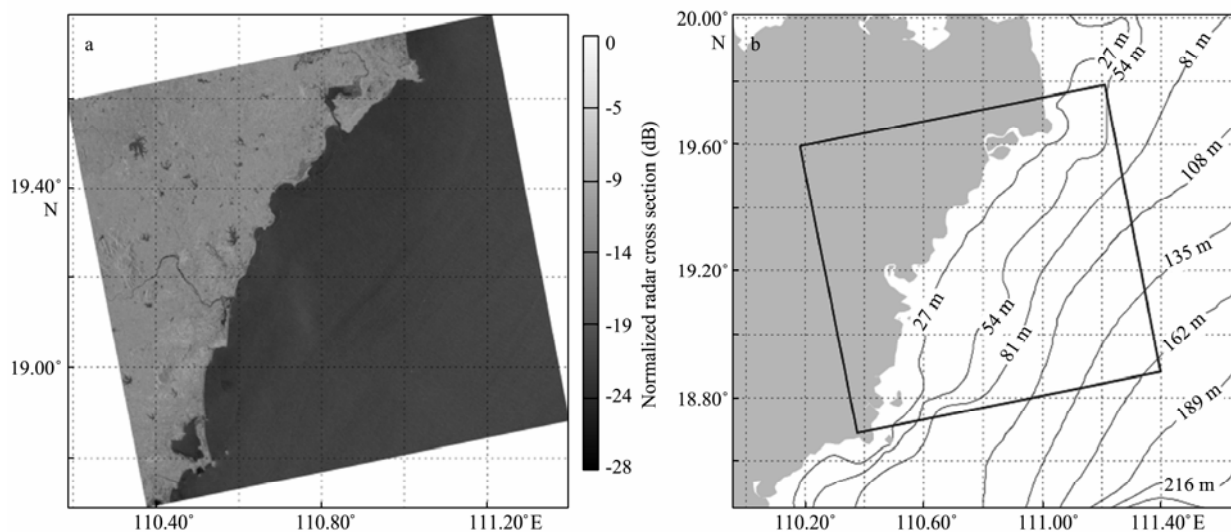


Fig.1 A case of RADARSAT2 SAR image taken on March 10th at 10:49 UTC in 2009 and the geographic location of the case of RADARSAT2 SAR image. (a) The case quick-look of the RADARSAT2 SAR image; (b) The geographic location of the case of RADARSAT2 SAR image. The levels are annotated by water depth and the black frame area is matched the full size of SAR image.

3 Methodology

3.1 CMOD Family of Geophysical Model Function

GMF is an empirical function developed for scatterometer at the beginning, and it is found that GMF is also suitable for retrieving wind field from SAR images (Lenher *et al.*, 1998; Monaldo *et al.*, 2001; Horstmann *et al.*, 2004; Zhang *et al.*, 2011) such as those for ERS SAR, RADARSAT SAR and ENVISAT ASAR. CMOD family models are developed aiming to retrieve wind field from C-band SAR images. The research made after several years of development for GMF (Offiler, 1994) showed that CMOD4 (Stoffelen and Anderson, 1992, 1997a, 1997b) was the most appropriate GMF for ERS-1 SAR. An important step is that CMOD5 was developed (Hersbach, 2003; Hersbach *et al.*, 2007), which was determined on the basis of a comparison of ERS-2 scatterometer triplet backscatter measurements with collocated ECMWF first-guess wind fields. During the tuning process, the formulation of CMOD5 is rigorously redesigned and linear higher-order wind speed corrections, which are neglected in CMOD4, are effectively implemented. Because of that, CMOD5 is more than an update version of its predecessor CMOD4 or CMOD-IFR2.

The relationship of CMOD family between the wind vector and normalized radar cross section takes the forms of

$$\sigma^0(U, \varphi) = A(\theta)U^{\gamma(\theta)}[1 + B(U, \varphi)\cos\varphi + C(U, \varphi)\cos 2\varphi] \quad (1)$$

where σ^0 represents normalized radar cross section, U is wind speed, φ represents the angle between the radar look direction and the wind direction ($\varphi=0$ means a wind blowing towards the radar and $\varphi=90$ means the wind direction crossing the radar beam), θ is the incidence angle, A , B , and C are parameters determined by sea surface wind conditions and γ is the function of incidence angle.

3.2 Foundation of Method

CMOD5 has been developed for correcting some deficiencies of the currently widely used CMOD4 GMF. Linear and higher-order wind speed corrections are rigorously implemented during the tuning process of CMOD5. The expression formulation such as that for A , B , C in Eq. (1) can be redesigned, and therefore CMOD5 is more than an update version of its predecessor, and is much flexible in possible future corrections. It is found that CMOD5 has a good performance of wind field retrieval under high wind speed condition (Quilfen *et al.*, 1998; Hortmann *et al.*, 2005; Shen *et al.*, 2006). However it does not mean that CMOD4 is not suitable to wind field retrieval. Oppositely, we found CMOD4 has a better performance than CMOD5 under low wind condition.

It is shown in Figs.2a-c) that CMOD5 has ambiguity of wind speed (black line) and a shape gradient of NRCS from low to moderate wind speed condition. Besides that

difference between CMOD4 and CMOD5 is significant only under low wind speed condition and pretty decreases when wind speed increases. That is the foundation of the method in our study.

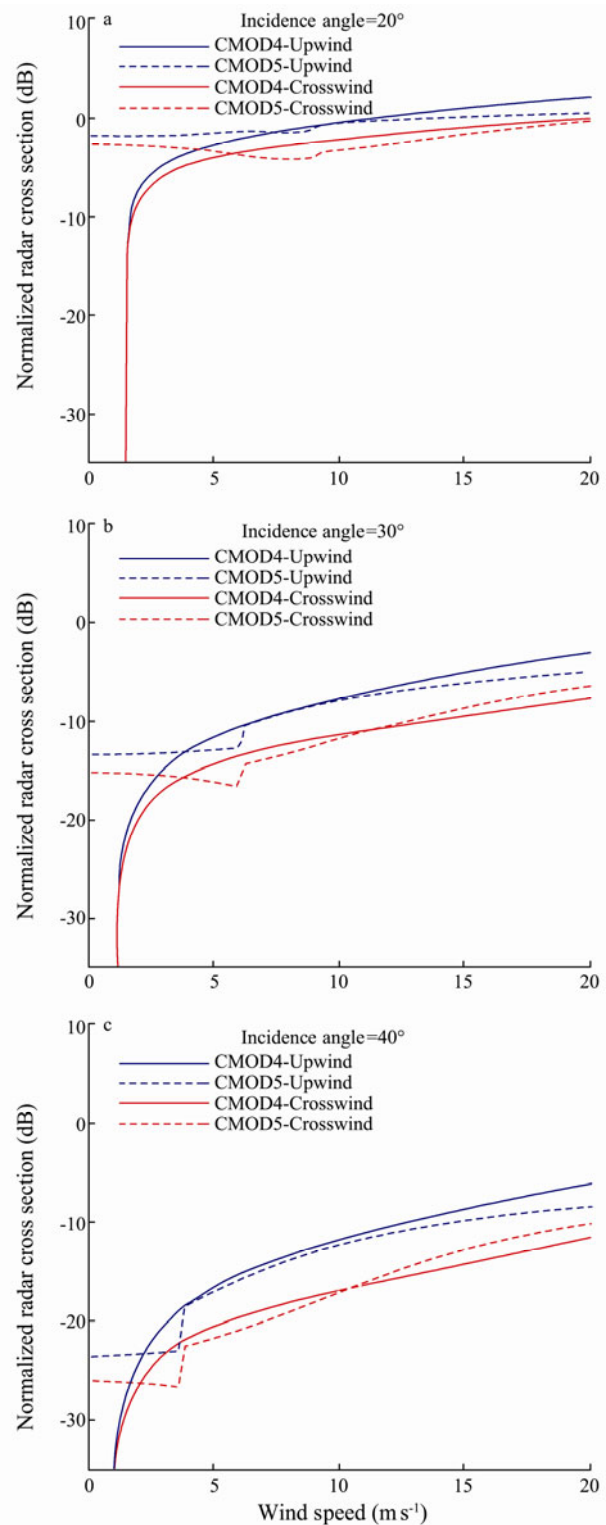


Fig.2 Performance of normalized radar cross section in CMOD4 and CMOD5 related to wind speed and wind direction. Upwind means wind direction is parallel to radar look direction. Crosswind means wind direction is perpendicular to radar look direction. (a) The incidence angle is 20°; (b) The incidence angle is 30°; (c) The incidence angle is 40°.

For avoiding this phenomenon, at first step CMOD5 is applied to simulate NRCS at fixed incidence angle and in prior wind direction. Instantaneously the gradient of NRCS is also calculated. And then it will clearly determine where the NRCS has a maximum gradient versus wind speed in the simulation. Corresponding to the maximum gradient, the spot is considered as the criterion to determine whether the observed NRCS has an ambiguity of wind speed. If observed NRCS is smaller than the criterion. CMOD4 is applied to wind speed retrieval. Oppositely, if observed NRCS is greater than the criterion. CMOD5 is used for wind speed retrieval. All process can be seen in Fig.3.

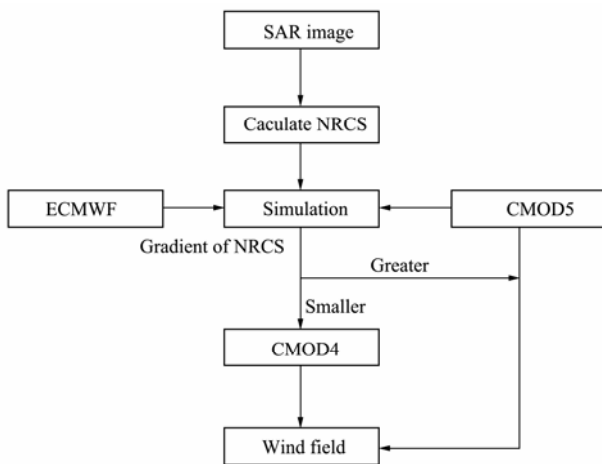


Fig.3 Flowchart of SAR wind field inversion.

3.3 Pretreatment of SAR Image

In this study, two CMOD models are used for inverting wind field. Before CMOD models are applied, it is necessary to derive normalized radar cross section from SAR images. Eq. (2) is taken for calculating normalized radar cross section from VV-polarisation RADARSAT2 SAR image:

$$\sigma^0 = \frac{DN^2}{DF} \times \sin \theta, \quad (2)$$

where σ^0 the normalized radar cross section; DN is the pixel value which can be reached from the SAR image directly and DF is the gain parameter of each pixel obtained directly from annotation file; θ is the incidence angle of each pixel.

In a SAR image, some atmospheric and marine phenomena such as wind, ocean slicks, ocean wave, etc, are mixed. They can affect normalized radar cross section, so it is necessary to minimize their influences in a SAR image. After calculating the normalized radar cross section of each pixel, average of normalized radar cross section of sub-images which are 256×256 pixels for eliminating other atmospheric and marine information is obtained. Finally, 40×40 sub-images of normalized radar cross section are derived.

A RADARSAT2 SAR image taken on March 17th at 10:45 UTC in 2009 is present as an example for retriev-

ing wind field by the method proposed in this paper.

3.4 External Wind Direction Information

Method using two-dimensional spectrum (SWDA: SAR wind direction algorithm) is widely used for estimation of wind direction. However, SWDA is difficult to be employed for derivation of wind direction from the SAR images where wind streak is not apparent. Because other ocean phenomena such as ocean slicks or fronts may deteriorate the image, leading to the misinterpretation of two-dimensional spectrum when searching for the spectrum peak related to wind streak. In our study, the SAR images were taken under low wind speed which is weak to produce homogenous wind streak. Therefore, in this paper, SWDA is not applicable for extracting wind direction information since the image lack apparent wind streak. We make use of ECMWF external wind direction as wind direction input. Fig.4 shows that ECMWF wind field acquired on March 17th at 12:00 UTC in 2009 which is nearest the time of example RADARSAT2 image. The technique proposed by Reppucci *et al.* (2008) for obtaining wind direction of each sub-image is used.

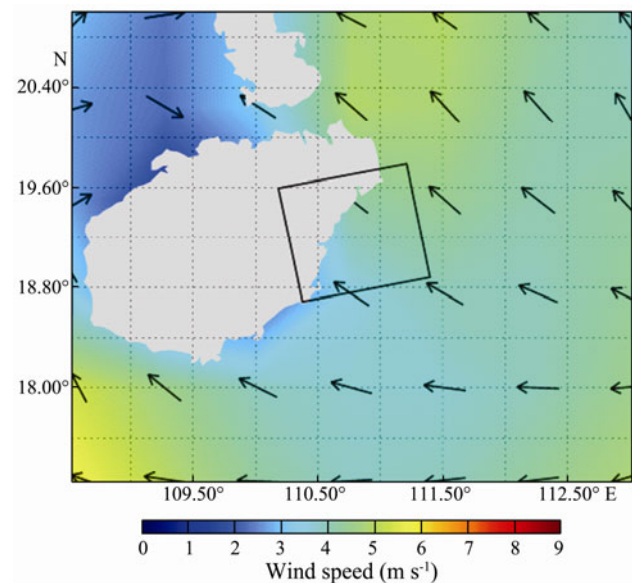


Fig.4 ECMWF wind field obtained at 12:00 UTC March 17th in 2009. Black box indicates the location of RADARSAT2 SAR image.

3.5 Inversion of Wind Speed

Comparison between retrieval results shows the feasibility of using CMOD4 and CMOD5 under moderate wind speed condition in practice with acceptable error. for both of them are considered capable of wind retrieval. Although it is found that CMOD4 and CMOD5 are much more similar under moderate wind speed condition than under low wind speed condition from simulation shown in Fig.2, CMOD5 has corrected some deficiencies of CMOD4. In this context, CMOD5 rather than CMOD4 is applied for wind speed retrieval when the observed NRCS is greater than criterion.

After getting interpolated wind direction from ECMWF wind field data using the technique proposed by Reppucci, wind speed is retrieved using CMOD family models. Because of the ambiguity in CMOD5, it is impossible to invert wind speed by CMOD5 GMF alone under low wind speed condition. The Fig.5 shows the results of an example of RADARSAT2 SAR image which are inverted by combined CMOD5 and CMOD4 and together with

CMOD4 GMF alone. The retrieval results with RADARSAT2 SAR image are compared those with QuikSCAT wind data as shown in Fig.6, the results being acquired for March 17th 2009 at 11:00 UTC in 2009. The retrieval results shown in Fig.5a obtained with the combination method are more accurate than those with by the single CMOD4 GMF alone as shown in Fig.5b, especially in the far range area where the wind speed is above 4 m s^{-1} .

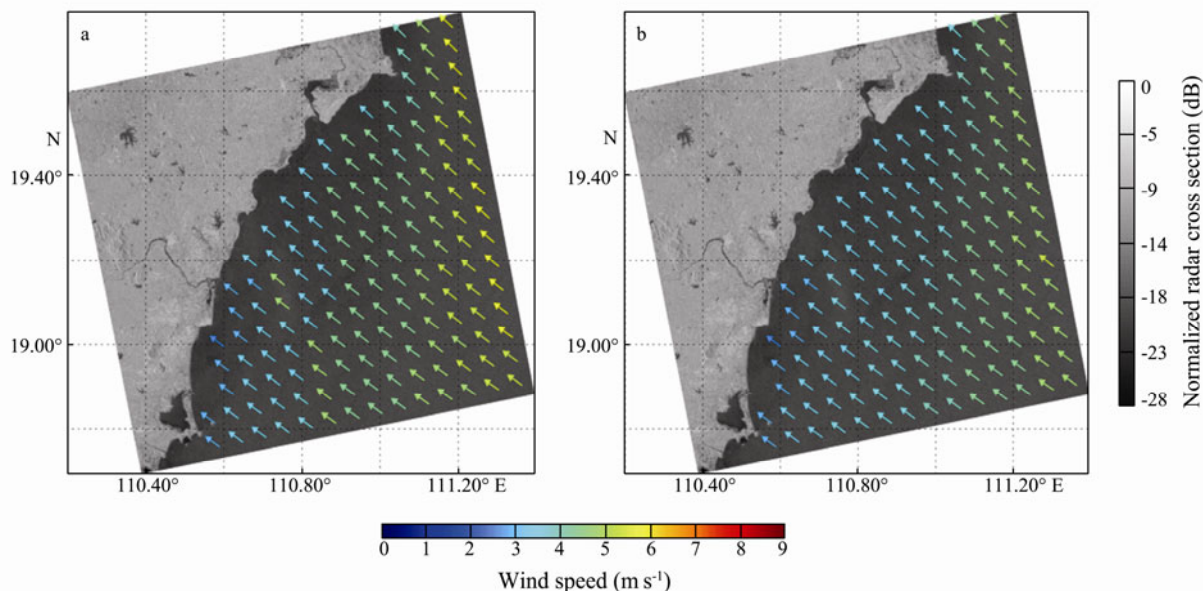


Fig.5 Sea surface wind field derived from RADARSAT2 SAR image taken on March 17th at 10:45 UTC in 2009 by CMOD5 and CMOD4, presented as an example. (a) Retrieval results by the combination method (CMOD5 and CMOD4); (b) Retrieval results by the single CMOD4 GMF alone.

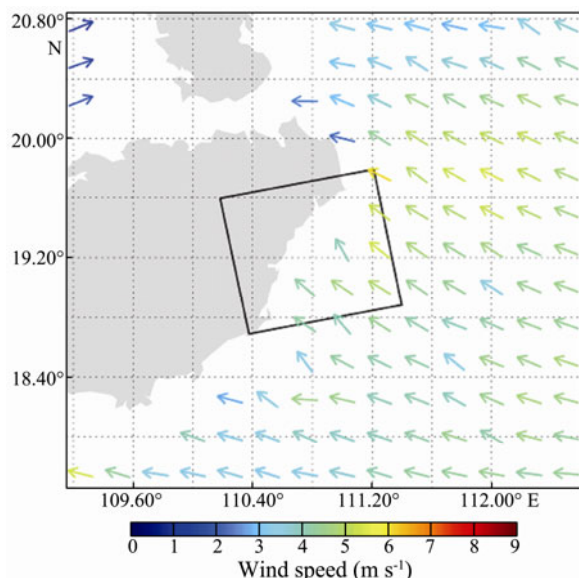


Fig.6 QuikSCAT wind field obtained at 05:00 UTC March 17th in 2009. Black box indicates the location of RADARSAT2 SAR image.

4 Analyses and Discussion

A total of 5 RADARSAT2 SAR images are implemented for validation in our study. The comparison of

wind speed derived from the combination method and from CMOD4 GMF alone with QuikSCAT wind speed is shown in Fig.7. The RMSE of wind speed is 0.75 m s^{-1} with correlation coefficient 0.84 by the combination method and the RMSE of wind speed is 1.01 m s^{-1} with correlation coefficient 0.72 using CMOD4 GMF alone for those cases.

The mean deviation of wind direction is limited within $\pm 20^\circ$ and that of wind speed is limited within $\pm 2 \text{ m s}^{-1}$ using SWDA+GMF. It is considered that the improved method proposed in this paper can be applicable for wind field retrieval from the SAR images where there is no apparent wind streak under low wind speed condition. It is noted that this method is not for developing the CMOD family but for retrieving practical wind field only. Therefore, the method has also the same shortcoming as in using SWDA+GMF.

5 Conclusions

In this paper an improved method was put into practice for retrieving wind field, and the method is based on two existing empirical geophysical model functions called CMOD family which can be applied directly for C-band SAR images. CMOD4 is widely used for retrieving wind field from C-band SAR images and CMOD5 has been developed recently by correcting some deficiencies of

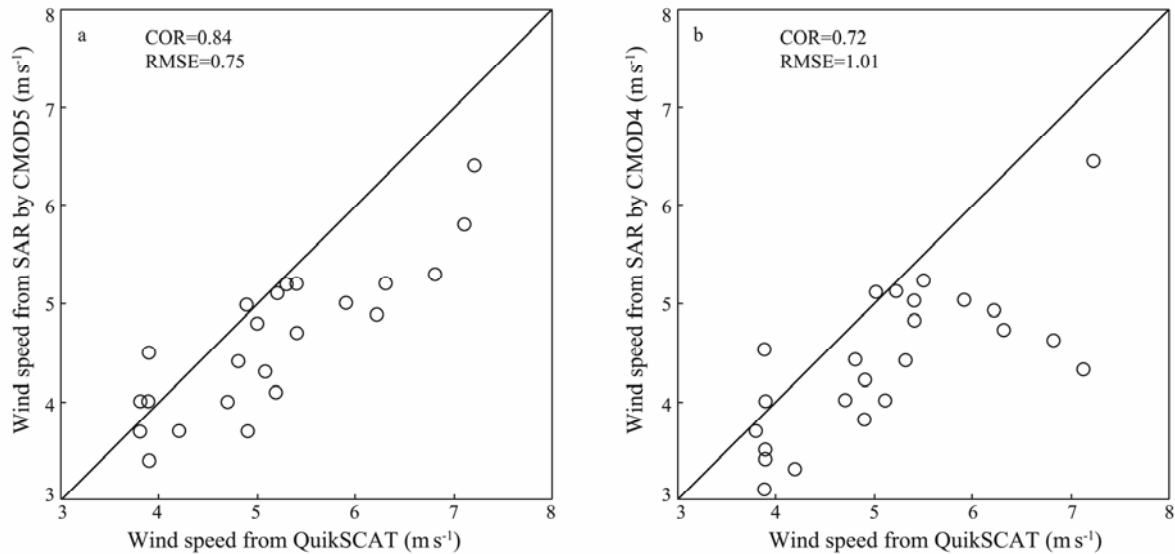


Fig.7 Scatter diagram representing the wind speed performance of the SAR inversion procedure. (a) Comparison between the combination method (CMOD5 and CMOD4) and QuikSCAT wind speed; (b) Comparison between the CMOD4 GMF alone and QuikSCAT wind speed.

CMOD4, which has a more fundamental basis. CMOD5 has wind speed ambiguity and large gradient of NRCS under low wind speed condition. In principle, the purpose of improved method is avoiding this internal defect of CMOD5 by calculating maximum gradient of NRCS in the simulation which is set as a criterion to determine whether CMOD5 is suitable to use for wind speed retrieval. If observed NRCS is smaller than the criterion, CMOD4 is applied to wind speed retrieval. If observed NRCS is greater than the criterion, CMOD5 is used for wind speed retrieval.

SWDA, which is widely used for estimation of wind direction, is not suitable for derivation of wind direction from SAR images where wind streak is not apparent. Because of that, $1.5^{\circ} \times 1.5^{\circ}$ ECMWF information is used as input wind direction. A total of 5 RADARSAT2 SAR images are implemented for validation. After comparing the results using the combination method (CMOD5 and CMOD4) to those using QuikSCAT wind speed, it is found that RMSE is 0.75 m s^{-1} with correlation coefficient 0.84 and the RMSE of wind speed is 1.01 m s^{-1} with correlation coefficient 0.72 using the CMOD4 GMF alone for those cases. It is concluded that the improved method can be used for wind field retrieval to avoid internal defect in CMOD5 under low wind speed condition.

Acknowledgements

RADARSAT2-SAR images were provided by Dr. Jian Sun. The authors appreciate the supports from the European Centre for Medium-Range Weather Forecasts (<http://www.ecmwf.int/research/era>) which supplies the $1.5^{\circ} \times 1.5^{\circ}$ wind direction information. QuikSCAT data comes from Physical Oceanography Distributed Active Archive Center (http://podaac.jpl.nasa.gov/order/order_qscat) which supplies the $0.25^{\circ} \times 0.25^{\circ}$ wind field information. This

study is supported by the National Natural Science Foundation of China (Nos. 41376010 and 40830959), and by the Start-up Foundation of Zhejiang Ocean University (No. 21105011913).

References

- Alpers, W., and Brummer, B., 1994. Atmospheric boundary layer rolls observed by the synthetic aperture radar aboard the ERS-1 satellite. *Journal of Geophysical Research*, **99** (C6): 12613-12621.
- Fetterer, F., Gimeris, D., and Wackerman, C. C., 1998. Validating a scatterometer wind algorithm for ERS-1 SAR. *IEEE Transactions on Geoscience and Remote Sensing*, **36**: 479-492.
- Gerling, T., 1986. Structure of the surface wind field from the Seasat SAR. *Journal of Geophysical Research*, **91** (C2): 2308-2320.
- Hersbach, H., 2003. *CMOD5: An Improved Geophysical Model Function for ERS C-band Scatterometry*. ECMWF Technical Memorandum No. 395, European Centre for Medium-Range Weather forecasts, 50pp.
- Hersbach, H., Stoffelen, A., and de Haan, S., 2007. An improved C-band scatterometer ocean geophysical model function: CMOD5. *Journal of Geophysical Research*, **112**: 3006-3024.
- Horstmann, J., Koch, W., and Lehner, S., 2004. Ocean wind fields retrieved from the advanced synthetic aperture radar aboard ENVISAT. *Ocean Dynamics*, **54**: 570-576, DOI: 10.1007/s10236-004-0098-3.
- Horstmann, J., Thompson, D. R., Monaldo, F., Iris, S., and Graber, H. C., 2005. Can synthetic aperture radars be used to estimate hurricane force winds? *Geophysical Research Letters*, **32**, L22801, DOI: 10.1029/2005GL023992.
- IFREMER, 1996. Off-line wind scatterometer ERS products: User Manual. Technical Report C2-MUT-W-01-IF, Version 2.0, IFREMER-CERSAT, Plouzane France, 75pp.
- Kerbaol, V., Chapron, B., and Vachon, P. W., 1998. Analysis of ERS-1/2 synthetic aperture radar wave Mode images. *Journal of Geophysical Research*, **103** (C4): 7833-7846.
- Koch, W., 2004. Directional analysis of SAR images aiming at

- wind direction. *IEEE Transaction on Geoscience and Remote Sensing*, **42**: 702-710.
- Lehner, S., Horstmann, J., Koch, W., and Rosenthal, W., 1998. Mesoscale wind measurements using recalibrated ERS SAR images. *Journal of Geophysical Research*, **103** (C4): 7847-7856.
- Monaldo, F., Thompson, D. R., Beal, R. C., Pichel, W. G., and Clemente-Colon, P., 2001. Comparison of SAR-derived wind speed with model predictions and buoy comparisons. *IEEE Transaction on Geoscience and Remote Sensing*, **39**: 2587-2600.
- Offiler, D., 1994. The calibration of ERS-1 satellite scatterometer winds. *Journal of Atmospheric and Oceanic Technology*, **11**: 1002-1017.
- Portabella, M., Stoffelen, A., and Johannessen, J. A., 2002. Toward an optimal inversion method for synthetic aperture radar wind retrieval. *Journal of Geophysical Research*, **107**: 1029-2001.
- Quilfen, Y., Chapron, B., and Elfouhaily, T., 1998. Observation of tropical cyclones by high-resolution scatterometry. *Journal of Geophysical Research-Oceans*, **103** (C4): 7767-7786.
- Reppucci, A., Lehner, S., Schulz-Stellenfleth J., and Yang C.S., 2008. Extreme wind conditions by satellite synthetic aperture radar in the North West Pacific. *International Journal of Remote Sensing*, **29** (21): 6129-6144.
- Shen, H., Perrie, W., and He, Y.-J., 2006. A new hurricane wind retrieval algorithm for SAR images, *Geophysical Research Letters*, **33**, L21812, DOI: 10.1029/2006GL027087.
- Shimada, T., and Kawamura, H., 2004. Wind jets and wind waves off Pacific coast of northern Japan under winter monsoon captured by combined use of scatterometer, synthetic aperture, and altimeter. *Journal of Geophysical Research-Oceans*, **109** (C12): 2004-2450.
- Stoffelen, A., and Anderson, D., 1992. ERS-1 scatterometer data and characteristics and wind retrieval skill. *European Space Agency Special Publication*, **359** (1): 41-47.
- Stoffelen, A., and Anderson, D., 1997a. Scatterometer data interpretation: Estimation and validation of the transfer function-CMOD4. *Journal of Geophysical Research*, **102**: 5767-5780.
- Stoffelen, A., and Anderson, D., 1997b. Scatterometer data interpretation: Measurement space and inversion. *Journal of Atmospheric and Oceanic Technology*, **14** (6): 1298-1313.
- Wacherman, C. C., Rufenach, C. L., Shuchman, R. A., Johannessen, J. A., and Davidson, K. L., 1996. Wind vector retrieval using ERS-1 synthetic aperture radar imagery. *IEEE Transaction on Geoscience and Remote Sensing*, **34**: 1343-1352.
- Zhang, B., Perrie, W., and He, Y.-J., 2011. Wind speed retrieval from RADARSAT-2 quad-polarization images using a new polarization ratio model. *Journal of Geophysical Research-Oceans*, **116**, C08008, DOI: 10.1029/2010JC006522.

(Edited by Xie Jun)